International Journal of Engineering Science 169 (2021) 103570

Contents lists available at ScienceDirect

International Journal of Engineering Science

journal homepage: www.elsevier.com/locate/ijengsci

Simultaneous recovery of transverse stresses at all points in a plate

R.C. Batra [*], B. Alanbay

Department of Biomedical Engineering and Mechanics, M/C 0219, Virginia Polytechnic Institute and State University, Blacksburg, VA 24061, USA

ARTICLE INFO

Keywords:
Stress recovery scheme
Principle of virtual work
Finite element method

ABSTRACT

We address the challenging issue of simultaneously finding transverse shear and normal stresses at all points in a plate from *a priori* known values of the in-plane stresses at plate's interior points. The principle of virtual work is employed to equate the work done by the transverse stresses to the difference between the work done by the external forces (applied surface tractions and body forces) and that by the in-plane stresses. The three transverse stresses and the virtual displacements are expressed in terms of polynomial (for example, those used in the finite element method) basis functions to deduce a system of simultaneous algebraic equations for the transverse stresses. The integrands for the right-hand side of these equations can be evaluated from the values of the in-plane stresses. The proposed scheme is advantageous over the current methods in economically evaluating accurate values of transverse stresses from the knowledge of the in-plane stresses at the Barlow points where they are most accurate. Since no spatial derivatives of the in-plane stresses are needed, this technique provides excellent values of transverse stresses. Results for three example problems are provided to illustrate the methodology and the accuracy of computed transverse stresses.

1. Introduction

Plates and shells have wide-ranging applications in civil, aerospace, and automotive industries. Analyses of their deformations using either an equivalent single layer (ESL) or a layer-wise (LW) theory for laminated and sandwich plates require fewer resources than those needed to study them as 3-dimensional structures. However, accurately ascertaining transverse stresses using displacement-based plate theories is rather challenging. Mixed plate theories that consider both displacements and stresses as variables and are based on Reissner's variational principle (Reissner, 1984) provide reasonable values of transverse stresses but have additional unknowns; e.g., see (Carrera, 2000). All six components of stresses are needed to use 3-dimensional failure criteria for determining the first failure load and the ultimate load a plate can support.

We now describe the scheme for finding transverse stresses as taught in a sophomore (2nd-year undergraduate at most US universities) level course on Mechanics of Deformable Bodies. Based on the assumptions that a thin beam of uniform cross-section having small width b and made of a homogeneous, isotropic and linearly elastic (i.e., Hookean) material undergoes infinitesimal plane-stress deformations and obeys kinematics of the Euler-Bernoulli theory, one derives an expression for the in-plane axial (bending) stress, $\sigma_{xx}\,(= -Mz/I_{yy})$ at a point P. As depicted in Fig. 1, the x-axis is along the beam length and passes through centroids of the cross-sections, M is the bending moment on the cross-section passing through P, z the distance of P from the neutral (or the centroidal) axis, and I_{yy} the 2nd moment of area of cross-section about the y-axis parallel to the beam width and passing through the cross-section

* Corresponding author.
E-mail address: rbatra@vt.edu (R.C. Batra).

https://doi.org/10.1016/j.ijengsci.2021.103570
Received 2 July 2021; Received in revised form 17 August 2021; Accepted 20 August 2021

centroid. As detailed in Section 5.5 of (Gere & Timoshenko, 1990), the equilibrium equation in the x-direction of an element $\Delta x \times t$ of the beam with one side coinciding with the top surface free of tangential tractions and of thickness t provides the transverse shear stress, σ_{xz} $(= VQ/(b\,I_{yy}))$ (Eq. 5.21 of (Gere & Timoshenko, 1990) where V is the shear force and Q the first moment of the area $b \times t$ about the y-axis. The equilibrium equation for this element in the z-direction gives $\sigma_{zz} = \mathrm{q} + \frac{\partial \sigma_{xz}}{\partial x}$ (neither derived in (Gere & Timoshenko, 1990) nor taught in the sophomore-level course). This is essentially the one-step stress recovery scheme (SRS). The shear stress σ_{xz} is a quadratic function of z, vanishes on the top and the bottom surfaces, varies quadrically over the beam height, and has the maximum value at the mid-surface.

For linearly elastic plates (or beams), the three partial differential equations of equilibrium are integrated with respect to the thickness co-ordinate z and the known traction boundary conditions on a major (either the top or the bottom) surface of the plate are used to recover the three transverse stresses at a point on the transverse normal to the plate. Note that the recovery of the transverse normal stress, σ_{zz}, requires that the first-order derivatives of the transverse shear stresses with respect to the in-plane co-ordinates (x and y) be reasonably accurate. The transverse shear stresses depend upon the first-order spatial derivatives of the in-plane stresses. Thus, second-order spatial derivatives of the in-plane stresses must be accurate to deduce reasonable values of the transverse normal stress. However, when using the first order shear deformation plate theory (FSDT) and low-order polynomial basis functions for the displacements, one gets at most accurate values of the in-plane stresses. Finding their spatial derivatives requires additional post-processing, such as using a finite-difference method on values of in-plane stresses at neighboring points. The numerical differentiation of in-plane stresses can introduce large errors.

We note that Chaudhuri and Seide (1987) employed 1-D quadratic shape functions through the thickness of each layer of the laminate to compute transverse shear stresses. Rohwer, Friedrichs, and Wehmeyer (2005) and Kant and Swaminathan (2000), amongst others, have reviewed different techniques to compute inter-laminar transverse stresses in laminates.

For transient deformations, one considers equations of motion that incorporate the inertia forces in the one-step SRS. To detect when failure initiates at a point requires using the SRS after every time step.

The accuracy of transverse stresses found with a one-step SRS can be improved upon by using a multi-step (or predictor-corrector) method, e.g., see Noor, Burton, and Peters (1990), Park and Kim (2002) and Park, Lee, and Kim (2003). In the predictor phase, Noor et al. (1990) found in-plane stresses from the FSDT displacements by including a shear correction factor and the transverse stresses with the SRS. The corrector phase is employed to improve upon the transverse stresses either by correcting the transverse shear stiffness or by modifying the through-the-thickness distribution of displacements to include both linear and non-linear terms. This

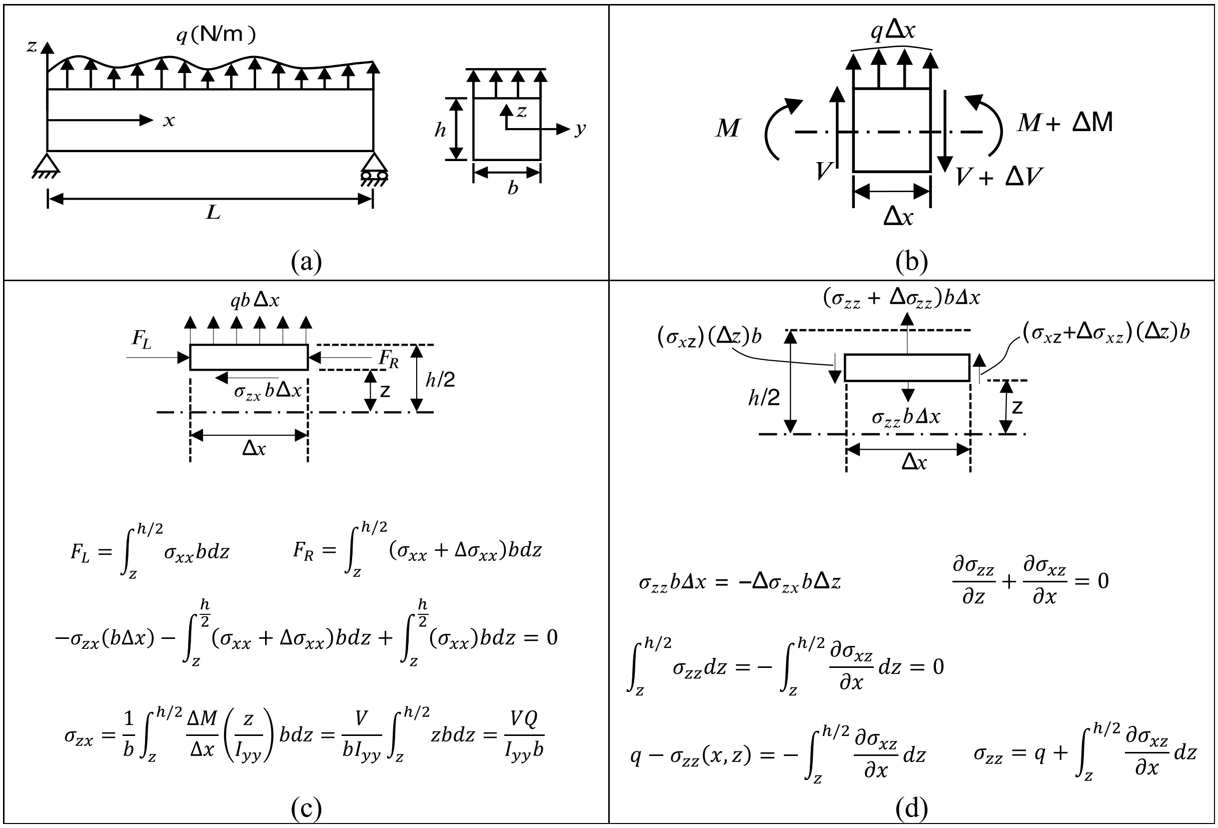

Fig. 1. (a) Sketch of a beam and of its side view, (b) Free body diagram of beam portion of length Δx, (c) Free body diagram of a section of length Δx and height $(h/2 - z)$, and (d) Free body diagram of a section of length Δx and height Δz in the beam interior.

iterative procedure is repeated till transverse stresses have converged within a prescribed tolerance.

For laminated structures analyzed with the ESL theories, one can improve upon the accuracy of the transverse stresses by incorporating the Murakami zig-zag function (Murakami, 1986) in the presumed through-the-thickness variation of the displacement field. Carrera (2000) has reviewed various plate theories and has compared their relative performances for laminates.

Shortcomings of the one-step SRS include (i) the need to have accurate values of 2nd order derivatives of the in-plane stresses with respect to in-plane co-ordinates, and (ii) for every point of interest in the plate the integration along a transverse normal starting from either the top or the bottom major surface to find transverse stresses there. Here we present a technique that overcomes these issues since it requires only values of in-plane stresses and simultaneously finds transverse stresses at all points. We note that the computation of in-plane stresses is not addressed in this work since it has been extensively studied in several books and research papers (too many to cite here). It relies on the principle of virtual work to equate the work done by the transverse stresses to the difference in the work done by the surface tractions applied on the bounding surface and the in-plane stresses. The integrands involving in-plane stresses can be evaluated from their values at the Barlow points (Barlow, 1976) within a finite element (FE) where they are more accurate than those at other points. Of course, one can also use values of the in-plane stresses at the Gauss integration points.

We note that in this work, the in-plane stresses are assumed to be *a priori* known. Accordingly, we neither discuss nor develop plate theories in this paper.

The rest of the paper is organized as follows. Algebraic equations for simultaneously finding transverse stresses at all nodes of a 3-dimensional FE mesh in the plate are derived in Section 2. These equations are modified to satisfy traction boundary conditions prescribed on plate's either the bottom or the top surface. Results for three example problems are illustrated in Section 3, and conclusions of the work are summarized in Section 4.

2. Problem formulation

We present the work for static infinitesimal deformations of a linearly elastic body and note that the procedure applies to plates comprised of functionally graded (or heterogeneous) materials. As shown in Fig. 2, we use rectangular Cartesian co-ordinates and denote the position vector of a material point by $\boldsymbol{x}$, with x_i denoting its component along the x_i- coordinate axis, $i = 1, 2, 3$. The x_3- axis is along the normal to the plate's two major (top and bottom) surfaces. A repeated index implies summation over the range of the index.

The stress field σ_{ij} for a body in equilibrium under the body force f_i per unit volume and surface tractions t_i on its bounding surfaces satisfies

$$\sigma_{ij,j} + f_i = 0, \text{ in } \Omega \tag{1}$$

$$\sigma_{ij}\, n_j = t_i, \text{ on } \partial\Omega \tag{2}$$

where Ω is the region occupied by the body, $\partial\Omega$ the boundary of Ω, $\boldsymbol{n}$ an outward unit normal to $\partial\Omega$, and $\sigma_{ij,j} = \partial\sigma_{ij}/\partial x_j$. At a free edge, $t_i = 0$. However, at either a clamped or a simply-supported edge, one or more components of t_i are unknown and are to be found as a part of the solution of the problem.

For the traction boundary-value problem (BVP) defined by Eqs. (1) and (2) to have a solution within a rigid body motion, the resultant force and moment about any point due to f_i and t_i must equal zero. Henceforth, we assume that these conditions are satisfied.

Assume that the plate theory equations using constitutive relations for the plate material, surface tractions t_i prescribed on plate's top and bottom surfaces and boundary conditions at the edge surfaces have been solved, and the in-plane stresses σ_{11}, σ_{22} and σ_{12} have been found everywhere in Ω. *Our objective is to find from σ_{11}, σ_{22} and σ_{12} the transverse stresses σ_{13}, σ_{23} and σ_{33} everywhere in Ω and, if needed, on the edge surfaces*. Note that the three equations (1) can be solved for only three unknowns. Thus the three in-plane stresses must be known to find the three transverse stresses.

2.1. Weak formulation of the problem

We assume that the region Ω has been discretized into N_e disjoint 3-dimensional (3D), not necessarily uniform, FEs Ω_e, $e = 1, 2,$

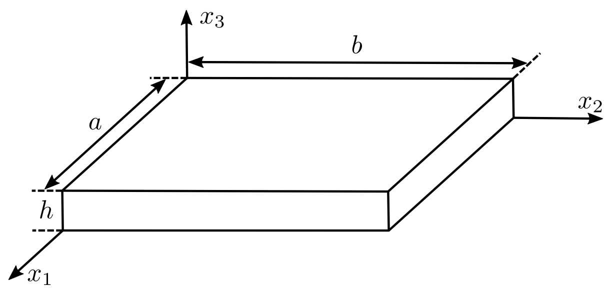

Fig. 2. Sketch of the problem studied.

$\ldots, N_e$, having a total of N_n nodes. We denote the N_n FE basis functions by $\psi_\alpha,\ \alpha = 1, 2, \ldots, N_n$. Recall that ψ_α equals 1 at node α and zero at the other nodes.

Consider a virtual displacement field

$$\phi^i = \psi_\alpha\, \delta d_\alpha^i \tag{3}$$

defined over Ω. In Eq. (3) the repeated index α is summed over its range $1, 2, \ldots, N_n$, $i = 1, 2, 3$, and δd_α^i equals the virtual displacement in the i^{th} direction of node α. The δd_α^i is not required to vanish anywhere on the boundary.

Taking the inner product of both sides of Eq. (1) with ϕ^i, integrating the resulting equation over Ω, using the divergence theorem on the term involving $\phi^i\,\sigma_{ij,j}$, and employing boundary condition (2), we arrive at

$$\int_\Omega \sigma_{ij}\phi^i_{,j}\, d\Omega = \int_\Omega f_i\phi^i d\Omega + \int_\Gamma t_i\phi^i\, d\Gamma \tag{4}$$

where $\Gamma = \partial\Omega$, $d\Gamma$ is an element of area on Γ and $d\Omega$ is a volume element in Ω. Eq. (4) states that during a virtual displacement ϕ^i, the work done by internal stresses σ_{ij} against the virtual strains produced by ϕ^i equals the sum of the work due to surface tractions t_i on all bounding surfaces of the plate and the body force f_i. Since $\sigma_{ij} = \sigma_{ji}$, we have

$$\int_\Omega \sigma_{ij}\phi^i_{,j}\, d\Omega = \int_\Omega \frac{1}{2}\sigma_{ij}\left(\phi^i_{,j} + \phi^j_{,i}\right) d\Omega \tag{5}$$

Substituting for ϕ^i from Eq. (3) into Eq. (4), recalling that δd_α^i is arbitrary, expressing the integral on Ω as the sum of integrals on Ω_e, and noting that σ_{11}, σ_{22} and σ_{12} are a priori known, we conclude from Eq. (4) the following.

$$\begin{aligned}&\sum_{e=1}^{e=N_e}\int_{\Omega e}\left(\sigma_{31}\left(\phi^3_{,1}+\phi^1_{,3}\right)+\sigma_{32}\left(\phi^3_{,2}+\phi^2_{,3}\right)+\sigma_{33}\,\phi^3_{,3}\right)d\Omega\\ &=\sum_{e=1}^{e=Ne}\left(\int_{\Gamma\cap\Omega_e} t_i\phi^i d\Gamma+\int_{\Omega_e} f_i\phi^i d\Omega-\int_{\Omega_e}\left(\sigma_{11}\phi^1_{,1}+\sigma_{12}\left(\phi^1_{,2}+\phi^2_{,1}\right)+\sigma_{22}\,\phi^2_{,2}\right)d\Omega\right)\end{aligned} \tag{6}$$

The integral in the first term on the right-hand side (RHS) of Eq. (6) is over all six surfaces of the rectangular plate. Surface tractions t_i on the top and the bottom surfaces are generally prescribed and hence are known, but those on the remaining four surfaces may be unknown, as discussed below after Eq. (9).

Using the FE basis functions, we write

$$\sigma_{3i}(x_1, x_2, x_3) = \psi_\alpha\, \sigma^\alpha_{3i},\ i = 1, 2, 3 \tag{7}$$

where σ^α_{3i} is the value of σ_{3i} at node α. Eq. (7) approximates a function in terms of a finite series, as is often done in the Fourier series method, where trigonometric (sines and cosines) are used as basis functions. Of course, any set of linearly independent basis functions can be used instead of trigonometric functions. Here we have used the FE basis functions for ease in evaluating the integrals involved and interpreting values of $\sigma_{3i}(x_1, x_2, x_3)$, $i = 1, 2, 3$. The quality of approximation depends upon the choice of basis functions and the number of terms kept in the series.

Substitution from Eqs. (3) and (7) into Eq. (6) and following the standard approach of numerically evaluating integrals over each Ω_e by using the appropriate Gauss quadrature rule, and assembling the element matrices into a global matrix as is done in a displacement-based approach (e.g., see (Becker, Carey, & Oden, 1981)), we arrive at

$$\boldsymbol{K}\,\widehat{\boldsymbol{\sigma}} = \boldsymbol{F} \tag{8}$$

where

$$\begin{aligned}K_{\alpha\beta i} &= \sum_{e=1}^{e=Ne}\int_{\Omega e}\left[\psi_\beta\left(\psi_{\alpha,1}+\psi_{\alpha,3}\right)\delta_{i1}+\psi_\beta\left(\psi_{\alpha,2}+\psi_{\alpha,3}\right)\delta_{i2}+\psi_\beta\,\psi_{\alpha,3}\delta_{i3}\right]d\Omega\\ \mathrm{F}_{i\alpha} &= \sum_{e=1}^{e=Ne}\left(\int_{\Gamma\cap\Omega_e} t_i\psi_\alpha d\Gamma+\int_{\Omega_e} f_i\psi_\alpha d\Omega-\int_{\Omega_e}\left(\left(\sigma_{11}\psi_{\alpha,1}+\sigma_{12}\psi_{\alpha,2}\right)\delta_{i1}+\left(\sigma_{12}\psi_{\alpha,1}+\sigma_{22}\psi_{\alpha,2}\right)\delta_{i2}\right)d\Omega\right)\\ \widehat{\boldsymbol{\sigma}} &= \left[\begin{array}{cccccccccc}\sigma^1_{31} & \sigma^1_{32} & \sigma^1_{33} & \sigma^2_{31} & \sigma^2_{32} & \sigma^2_{33} & \cdots & \sigma^{Nn}_{31} & \sigma^{Nn}_{32} & \sigma^{Nn}_{33}\end{array}\right]^T\end{aligned} \tag{9}$$

In Eq. (9) δ_{ij} is the Kronecker delta having values 1 for $i = j$ and zero otherwise. Note that for $i = 1, 2, 3$, the matrix $K_{\alpha\beta i}$ is not symmetric. The integrals in the expression for the force $\boldsymbol{F}$ can be evaluated by using an appropriate Gauss quadrature rule and values of stresses σ_{11}, σ_{12} and σ_{22} at either the integration or the Barlow points (Barlow, 1976) where they are most accurate. Alternatively, one can employ their values at the nodes, and use nodes as integration points, i.e., adopt Lobatto's quadrature rule. The integrals in the expression for $\boldsymbol{K}$ can be evaluated as usual by using the appropriate Gauss quadrature rule.

We now rewrite Eqs. (9) to facilitate the software development. Recalling that the restriction of the FE basis functions to an element gives shape functions $\boldsymbol{N}$ for nodes on the element, we write the matrix $\boldsymbol{K}$ of Eq. (9) as

$$\boldsymbol{K} = \sum_{e=1}^{e=Ne} \int_{\Omega_e} \boldsymbol{B}_{\mathbf{n}}^{\mathrm{T}} \boldsymbol{N} d\Omega \tag{10}$$

where

$$\boldsymbol{B}_{\mathbf{n}} = [\boldsymbol{B}_{\mathbf{n1}} \quad \boldsymbol{B}_{\boldsymbol{n2}} \quad \ldots \quad \boldsymbol{B}_{\mathbf{N_nN_n}}\ ],\ \boldsymbol{B}_{\mathbf{n}\boldsymbol{\alpha}} = \begin{bmatrix} \psi_{\alpha,3} & 0 & \psi_{\alpha,1} \\ 0 & \psi_{\alpha,3} & \psi_{\alpha,2} \\ 0 & 0 & \psi_{\alpha,3} \end{bmatrix} \tag{11}$$

$$\boldsymbol{N} = [\mathbf{N_1} \quad \mathbf{N_2} \quad \cdots \quad \boldsymbol{N}_{\mathbf{N_n}}\ ],\ \boldsymbol{N}_{\boldsymbol{\alpha}} = \begin{bmatrix} \psi_\alpha & 0 & 0 \\ 0 & \psi_\alpha & 0 \\ 0 & 0 & \psi_\alpha \end{bmatrix} \tag{12}$$

Similarly, we write the force vector $\boldsymbol{F}$ in Eq. (9) as

$$\boldsymbol{F} \ = \sum_{e=1}^{e=Ne} \left(\int_{\Gamma\cap\Omega_e} \boldsymbol{N}^{\mathrm{T}} \boldsymbol{t}\ d\Gamma + \int_{\Omega_e} \boldsymbol{N}^{\mathrm{T}} \boldsymbol{f} d\Omega - \int_{\Omega_e} \boldsymbol{B}_{\mathbf{p}} \begin{Bmatrix} \sigma_{11} \\ \sigma_{22} \\ \sigma_{12} \end{Bmatrix} d\Omega \right) \tag{13}$$

where

$$\boldsymbol{B}_{\mathbf{p}} = [\mathbf{B_{p1}} \quad \mathbf{B_{p2}} \quad \cdots \quad \boldsymbol{B}_{\mathbf{pn}}\ ],\ \boldsymbol{B}_{\mathbf{p}\boldsymbol{\alpha}} = \begin{bmatrix} \psi_{\alpha,1} & 0 & 0 \\ 0 & \psi_{\alpha,2} & 0 \\ \psi_{\alpha,2} & \psi_{\alpha,1} & 0 \end{bmatrix} \tag{14}$$

For a rectangular plate, the first term on the RHS of Eq. (13) equals the sum on all six bounding surfaces as illustrated below.

$$\begin{gathered} \int_{\Gamma\cap\Omega_e} \boldsymbol{N}^{\mathrm{T}} \boldsymbol{t}\ d\Gamma = \\ \int_{\Gamma_1} \boldsymbol{N}^{\mathrm{T}} \begin{Bmatrix} \sigma_{11} \\ \sigma_{21} \\ \sigma_{31} \end{Bmatrix} d\Gamma - \int_{\Gamma_2} \boldsymbol{N}^{\mathrm{T}} \begin{Bmatrix} \sigma_{11} \\ \sigma_{21} \\ \sigma_{31} \end{Bmatrix} d\Gamma + \int_{\Gamma_3} \boldsymbol{N}^{\mathrm{T}} \begin{Bmatrix} \sigma_{12} \\ \sigma_{22} \\ \sigma_{32} \end{Bmatrix} d\Gamma - \int_{\Gamma_4} \boldsymbol{N}^{\mathrm{T}} \begin{Bmatrix} \sigma_{12} \\ \sigma_{22} \\ \sigma_{32} \end{Bmatrix} d\Gamma + \int_{\Gamma_5} \boldsymbol{N}^{\mathrm{T}} \begin{Bmatrix} \sigma_{31} \\ \sigma_{32} \\ \sigma_{33} \end{Bmatrix} d\Gamma - \\ \int_{\Gamma_6} \boldsymbol{N}^{\mathrm{T}} \begin{Bmatrix} \sigma_{31} \\ \sigma_{32} \\ \sigma_{33} \end{Bmatrix} d\Gamma \end{gathered} \tag{15}$$

Here Γ_1, Γ_2, Γ_3, Γ_4, Γ_5, and Γ_6 , respectively, correspond to the edges $x_1 = a$, $x_1 = 0$, $x_2 = b$, $x_2 = 0$, $x_3 = h$, and $x_3 = 0$. Surface tractions prescribed on the top (Γ_5) and the bottom (Γ_6) surfaces are denoted below in Eq. (18) with a superimposed bar. Substituting from Eq. (15) into Eq. (9) and transferring terms involving σ_{i3} on surfaces Γ_1, Γ_2, Γ_3, Γ_4 from the RHS to the LHS we get

$$\boldsymbol{K}_{\mathrm{S}}\, \boldsymbol{\sigma} \ = \ \boldsymbol{F}_{\mathrm{S}} \tag{16}$$

where

$$\begin{gathered} \boldsymbol{K}_{\mathrm{S}} = \\ \sum_{e=1}^{e=Ne} \left(\int_{\Omega_e} \boldsymbol{B}_{\mathbf{n}}^{\mathrm{T}} \boldsymbol{N} d\Omega + \int_{\Gamma_1\cap\Omega_e} \boldsymbol{N}^T \begin{bmatrix} 0 & 0 & 0 \\ 0 & 0 & 0 \\ 1 & 0 & 0 \end{bmatrix} \boldsymbol{N} d\Gamma + \int_{\Gamma_2\cap\Omega_e} \boldsymbol{N}^T \begin{bmatrix} 0 & 0 & 0 \\ 0 & 0 & 0 \\ 1 & 0 & 0 \end{bmatrix} \boldsymbol{N} d\Gamma - \right. \\ \left. \int_{\Gamma_3\cap\Omega_e} \boldsymbol{N}^{\mathrm{T}} \begin{bmatrix} 0 & 0 & 0 \\ 0 & 0 & 0 \\ 0 & 1 & 0 \end{bmatrix} \boldsymbol{N} d\Gamma + \int_{\Gamma_4\cap\Omega_e} \boldsymbol{N}^T \begin{bmatrix} 0 & 0 & 0 \\ 0 & 0 & 0 \\ 0 & 1 & 0 \end{bmatrix} \boldsymbol{N} d\Gamma \right) \end{gathered} \tag{17}$$

and

$$\boldsymbol{F}_{\mathbf{S}}=\sum_{e=1}^{e=Ne}\left(\int_{\Omega_e}\boldsymbol{N}^{\mathrm{T}}fd\Omega-\int_{\Omega_e}\boldsymbol{B}_{\mathbf{p}}\left\{\begin{matrix}\sigma_{11}\\ \sigma_{22}\\ \sigma_{12}\end{matrix}\right\}d\Omega+\int_{\Gamma_1}\boldsymbol{N}^{\mathrm{T}}\left\{\begin{matrix}\sigma_{11}\\ \sigma_{21}\\ 0\end{matrix}\right\}d\Gamma-\int_{\Gamma_2}\boldsymbol{N}^{\mathrm{T}}\left\{\begin{matrix}\sigma_{11}\\ \sigma_{21}\\ 0\end{matrix}\right\}d\Gamma\right.$$
$$+\int_{\Gamma_3}\boldsymbol{N}^{\mathrm{T}}\left\{\begin{matrix}\sigma_{12}\\ \sigma_{22}\\ 0\end{matrix}\right\}d\Gamma-\int_{\Gamma_4}\boldsymbol{N}^{\mathrm{T}}\left\{\begin{matrix}\sigma_{12}\\ \sigma_{22}\\ 0\end{matrix}\right\}d\Gamma+\int_{\Gamma_5}\boldsymbol{N}^{\mathrm{T}}\left\{\begin{matrix}\overline{\sigma}_{13}\\ \overline{\sigma}_{23}\\ \overline{\sigma}_{33}\end{matrix}\right\}d\Gamma \tag{18}$$
$$\left.-\int_{\Gamma_6}\boldsymbol{N}^{\mathrm{T}}\left\{\begin{matrix}\overline{\sigma}_{13}\\ \overline{\sigma}_{23}\\ \overline{\sigma}_{33}\end{matrix}\right\}d\Gamma\right)$$

After having found nodal values of σ_{i3}, the transverse stresses at any other point are computed from Eq. (7). It is clear that values of the in-plane stresses and not their spatial derivatives are needed to evaluate the RHS of Eq. (16), and transverse stresses at all nodes are simultaneously computed. The FE mesh can be refined to improve upon the accuracy of σ_{i3}. Furthermore, a non-uniform FE mesh with smaller elements near the plate edges should give better estimates of σ_{i3} at points close to the edges.

3. Example problems

In the three example problems discussed below, we have discretized the rectangular plate domain into 8-node brick elements and employed $2 \times 2 \times 2$ Gauss quadrature rule to numerically evaluate the integrals. The integrals over the 4-node elements on the plate edge surfaces have been evaluated with the 2×2 Gauss quadrature rule. In Eq. (16) values of surface tractions prescribed on the bottom surface, $x_3 = 0$, are enforced by modifying the relevant equations using the penalty method.

3.1. *Arbitrary loading of a plate (or the method of manufactured solutions)*

For the rectangular plate exhibited in Fig. 2, we set $a = b = 1$ m, $h = 0.1$ m, and use the method of manufactured solutions (MMS) (e.g., see the material following Eq. 20 of (Batra & Liang, 1997) and elaborated upon on page 759 of (Batra & Love, 2005), wherein it is called the method of fictitious body forces) to find an analytical solution of a problem. The method entails assuming a displacement field (i.e., the solution) and finding body forces and surface tractions required to produce it. For the displacement field

$$u_1 = x_1x_2x_3,\ u_2 = (1-x_1)(1-x_2)x_3,\ u_3 = x_1(1-x_3)(1-x_2) \tag{19}$$

we find the corresponding infinitesimal strains by using the strain-displacement relations, and then stresses by using the constitutive relation (Hooke's law) for an isotropic and homogeneous plate with Young's modulus $E = 70$ GPa, and Poisson's ratio $\nu = 0.3$. Substitution for stresses in the equilibrium Eq. (1) and boundary condition Eq. (2) provides the body force and tractions on the six bounding surfaces for the displacement field Eq. (19) to occur in the plate; expressions for the stresses, boundary conditions and surface tractions are given in the Appendix. Values of surface tractions t_i in Eq. (2) on surfaces $\Gamma_1,\ \Gamma_2,\ \Gamma_3,\ \Gamma_4$ and Γ_5 are employed in the RHS of Eq. (16) and those on Γ_6 are enforced by the penalty method. Values of transverse stresses at some interior points computed by using the $20 \times 20 \times 10$ FE mesh (i.e., 20, 20 and 10 elements, respectively, in the x_1-, the x_2-, and the x_3- directions) are compared in Table 1 and Table 2 with those from the MMS. It is evident that there is an excellent agreement between the SRS and the analytical transverse stresses.

Table 1
Comparison of through-the-thickness transverse stresses (Unit: GPa).

x_3	Analytical			SRS		
	[a]$\widehat{\sigma}_{13}$	[a]$\widehat{\sigma}_{23}$	[a]$\widehat{\sigma}_{33}$	[a]$\widehat{\sigma}_{13}$	[a]$\widehat{\sigma}_{23}$	[a]$\widehat{\sigma}_{33}$
0	14.14	−0.67	−17.67	14.14	−0.67	−17.67
0.01	14.00	−0.54	−17.87	14.00	−0.54	−17.87
0.02	13.87	−0.40	−18.07	13.87	−0.40	−18.07
0.03	13.73	−0.27	−18.27	13.73	−0.27	−18.27
0.04	13.60	−0.13	−18.48	13.60	−0.13	−18.48
0.05	13.46	0.00	−18.68	13.46	0.00	−18.68
0.06	13.33	0.13	−18.88	13.33	0.13	−18.88
0.07	13.19	0.27	−19.08	13.19	0.27	−19.08
0.08	13.06	0.40	−19.28	13.06	0.40	−19.28
0.09	12.92	0.54	−19.49	12.92	0.54	−19.49
0.1	12.79	0.67	−19.69	12.79	0.67	−19.69

[a] $[\widehat{\sigma}_{13}(x_3), \widehat{\sigma}_{23}(x_3),\ \widehat{\sigma}_{33}(x_3)] = [\sigma_{13}(0.05,\ 0.5,\ x_3),\ \sigma_{23}(0.5,\ 0.05, x_3),\ \sigma_{33}(0.25,\ 0.25, x_3)]$

Table 2
Comparison of transverse stresses at points along the line $x_1 = 0.5$ m, $x_3 = 0.05$ m (Unit: GPa).

	Analytical			SRS		
x_2	$\hat{\sigma}_{13}$	$\hat{\sigma}_{23}$	$\hat{\sigma}_{33}$	$\hat{\sigma}_{13}$	$\hat{\sigma}_{23}$	$\hat{\sigma}_{33}$
0	25.58	0.67	−48.13	25.58	0.67	−48.13
0.1	24.37	−0.67	−43.21	24.37	−0.67	−43.21
0.2	23.15	−2.02	−38.30	23.15	−2.02	−38.30
0.3	21.94	−3.37	−33.39	21.94	−3.37	−33.39
0.4	20.73	−4.71	−28.47	20.73	−4.71	−28.47
0.5	19.52	−6.06	−23.56	19.52	−6.06	−23.56
0.6	18.31	−7.40	−18.64	18.31	−7.40	−18.64
0.7	17.10	−8.75	−13.73	17.10	−8.75	−13.73
0.8	15.89	−10.10	−8.82	15.89	−10.10	−8.82
0.9	14.67	−11.44	−3.90	14.67	−11.44	−3.90
1	13.46	−12.79	1.01	13.46	−12.79	1.01

3.2. Simply-supported 45° fiber-reinforced lamina

As a second example problem, we study deformations of a $1 \times 1 \times 0.2$ m^3 simply supported 45° fiber-reinforced graphite/epoxy lamina subjected to the sinusoidal load, $q_0 \sin(\pi x_1/a) sin(\pi x_2/b)$, perpendicular to the top surface and having following values of the material parameters): $E_1 = 132.5$ GPa, $E_2 = E_3 = 10.8$ GPa, $G_{12} = G_{13} = 5.7$ GPa, $G_{23} = 3.4$ GPa, $\nu_{12} = \nu_{13} = 0.24$, and $\nu_{23} = 0.49$. The problem is analytically solved using Srinivasa and Rao's approach (Srinivas & Rao, 1970), and the in-plane stresses so found are used to compute the RHS of Eq. (16). In Table 3 we have compared the normalized transverse stresses

$$\left[\hat{\sigma}_{13}, \hat{\sigma}_{23}, \ \hat{\sigma}_{33}\right] = \frac{1}{q_0}[\sigma_{13}(0.1a, \ 0.5b, \ 0.5h), \ \sigma_{23}(0.5a, \ 0.1b, \ 0.5h), \ \sigma_{33}(0.5a, \ 0.5b, \ 0.5h)]$$

computed using various FE meshes with their values from the analytical solution. It is clear that with the FE mesh refinement, the SRS results converge to the analytical solution. Except for the $80 \times 80 \times 4$ and $80 \times 80 \times 6$ FE meshes, the SRS transverse stresses differ from their analytical values by less than 1%.

Fig. 3 shows through-the-thickness distributions of the transverse shear stresses σ_{13} and σ_{23} near the edges $x_1 = 0$ and $x_2 = 0$, and of the transverse normal stress σ_{33} at the plate center. The black dashed lines and red "+" markers, respectively, correspond to the SRS and the analytical solution. The SRS results are in excellent agreement with those of the analytical solution.

3.3. Two-layer [0°/90°] laminate

The efficiency of the proposed SRS scheme to calculate transverse stresses is investigated for a simply-supported square [0°/90°] laminate having the same geometry, loading and material properties as that for the lamina in Section 3.2. This problem is also analytically solved with Srinivas and Rao's approach. It is evident from the plots exhibited in Fig. 4 of the through-the-thickness distributions of the SRS computed transverse stresses using the $60 \times 60 \times 30$ uniform FE mesh and their values from the analytical solution that two sets of results are in excellent agreement with each other and the transverse stresses are continuous across the interface between the two layers.

Remarks:

Recall that the methodology presented here for simultaneously recovering transverse stresses at all points in a plate only requires values of in-plane Cauchy stresses and the deformed shape of the plate. Thus, it applies to finite deformation problems.

No step in the derivation of the procedure requires that the plate be made of either an isotropic or a homogeneous material. Since in-plane stresses are *a priori* known, the inhomogeneity of the material properties has been considered in evaluating them. The

Table 3
Convergence of transverse stresses in a square simply-supported transversely isotropic lamina (FE Mesh $60 \times 80 \times 20$ represents 60, 80 and 20 elements in the x_1-, the x_2-, and the x_3- directions, respectively).

FE Mesh	$\hat{\sigma}_{13}$	$\hat{\sigma}_{23}$	$\hat{\sigma}_{33}$		$\hat{\sigma}_{13}$	$\hat{\sigma}_{23}$	$\hat{\sigma}_{33}$
20 × 20 × 20	1.7561	0.4506	0.5017	80 × 80 × 4	1.6749	0.4429	0.5467
40 × 40 × 20	1.7507	0.4492	0.5002	80 × 80 × 6	1.8402	0.4675	0.4749
60 × 60 × 20	1.7497	0.4490	0.4999	80 × 80 × 10	1.7848	0.4558	0.4893
80 × 80 × 20	1.7494	0.4489	0.4998	80 × 80 × 20	1.7494	0.4489	0.4998
100 × 100 × 20	1.7492	0.4488	0.4998	80 × 80 × 30	1.7562	0.4499	0.4967
120 × 120 × 20	1.7491	0.4488	0.4997	80 × 80 × 40	1.7518	0.4491	0.4982
Analytical	**1.7522**	**0.4490**	**0.4976**				

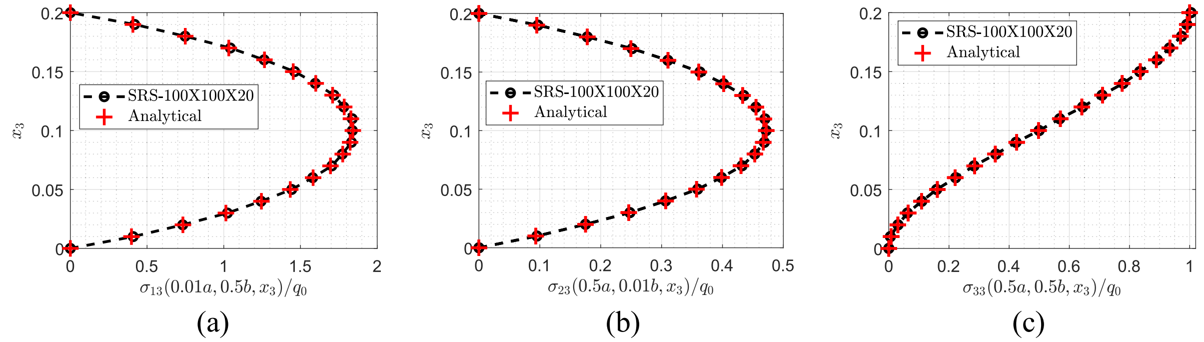

Fig. 3. Through-the-thickness distributions of the transverse stresses: a) σ_{13}, b) σ_{23}, and c) σ_{33} for a simply-supported square transversely isotropic lamina.

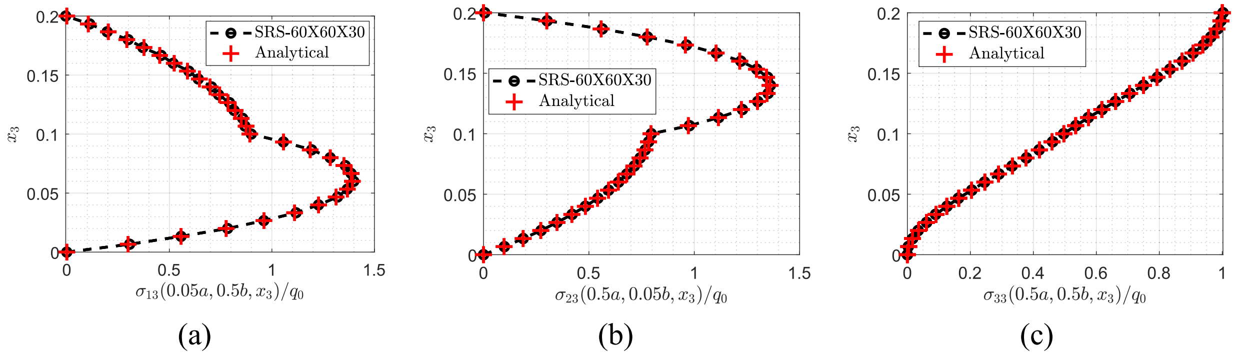

Fig. 4. Through-the-thickness distributions of the transverse stresses: a) σ_{13}, b) σ_{23}, and c) σ_{33} for a square [0°/90°] laminate.

computation of transverse stresses requires only using the principle of virtual work, which is applicable to a heterogeneous and anisotropic plate.

The problem formulation uses the divergence theorem in deriving Eq. (4). Thus, it is applicable to a plate occupying a *normal* region (see Section 2, page 85 of (Kellog, 1953)) in the reference (deformed) configuration for infinitesimal (finite) deformations.

For plates of variable thickness, the FE mesh, in general, will not have uniform elements. In the FE method, one usually maps a FE onto a master element and performs integrations over the master element. The Jacobian of the mapping from the master element onto the actual FE will have different values at the Gauss quadrature points. For a sufficiently refined FE mesh and an appropriate number of quadrature points, these integrals can be evaluated to the desired accuracy. Furthermore, the plate region can be subdivided into hexahedral elements.

Other basis functions such as those derived by the moving least squares approximation can be employed in place of the FE basis functions. A FE basis function associated with a node equaling one there and zero at the remaining nodes facilitates the interpretation of the computed transverse stresses.

Even though we have presented results for a rectangular plate, the methodology is applicable to circular and polygonal plates. The accuracy of the recovered transverse stresses near the corners will depend upon that of the in-plane stresses there. We hope to present results for these plates and for finite deformation problems in future studies.

4. Conclusions

We have developed a novel one-step stress recovery scheme (SRS) that does not require spatial derivatives of in-plane stresses and simultaneously provides values of transverse stresses at all points in the plate domain. It uses the principle of virtual work to equate the work done by the transverse stresses to the difference between that done by the applied surface tractions and the in-plane stresses. Using the finite element (FE) basis functions (or any other set of linearly independent basis functions defined on the plate domain), one can derive a set of simultaneous algebraic equations for the three transverse stresses at the nodes. These algebraic equations are modified to satisfy the applied surface tractions on either the bottom or the top surface of the plate. The accuracy of the computed transverse stresses can be enhanced by refining the FE mesh. The technique is highly versatile since it is applicable to all regions for which the divergence theorem is applicable. It is robust since it simultaneously finds the three transverse stresses at all plate points. It can be easily incorporated into a commercial FE software. Significant advantages of the proposed technique include using values of only in-plane stresses at the integration points, and finding transverse stresses simultaneously at all points of the plate.

Declaration of Competing Interest

The authors declare no conflict of interest.

Acknowledgments

The financial support of the work from the U.S. Office of Naval Research (ONR) through grants N00014-18-1-2548, N00014-20-1-2876, and N00014-21-1-2283 with Y. D. S. Rajapakse as the Program Manager, to Virginia Polytechnic Institute and State University (Virginia Tech) is gratefully acknowledged. Views expressed in the paper are those of the authors and neither of the funding agency nor of Virginia Tech.

Appendix

We list below expressions for the stresses, the body forces, and the surface tractions obtained from the displacement field listed as Eq. (19) in Section 3.1.

Stresses:

$$\sigma_{11}(x_1,x_2,x_3) = (1543876923076923x_2x_3)/16384 + (132332307692307x_1(x_2-1))/32768 + (1323323076923077x_3(x_1-1))/32768$$

$$\sigma_{22}(x_1,x_2,x_3) = (1323323076923077x_2x_3)/32768 + (1323323076923077x_1(x_2-1))/32768 + (1543876923076923x_3(x_1-1))/16384$$

$$\sigma_{33}(x_1,x_2,x_3) = (1323323076923077x_2x_3)/32768 + (1543876923076923x_1(x_2-1))/16384 + (1323323076923077x_3(x_1-1))/32768$$

$$\sigma_{13}(x_1,x_2,x_3) = (7057723076923077(x_1-1)(x_2-1))/262144 + (7057723076923077x_1(x_3-1))/262144$$

$$\sigma_{23}(x_1,x_2,x_3) = (7057723076923077(x_2-1)(x_3-1))/262144 + (7057723076923077x_1x_2)/262144$$

Body Forces:

$$f_1(x_1,x_2,x_3) = 17644307692307693/262144 - (17644307692307693x_3)/262144 - (17644307692307693x_2)/262144$$

$$f_2(x_1,x_2,x_3) = -(17644307692307693x_1)/262144 - (17644307692307693x_3)/262144$$

$$f_3(x_1,x_2,x_3) = 17644307692307693/262144 - (17644307692307693x_2)/262144 - (17644307692307693x_1)/262144$$

Surface Tractions

Left edge surface, $x_1 = 0$

$$\sigma_{11}(0,x_2,x_3) = (1323323076923077x_3)/32768 - (1543876923076923x_2x_3)/16384$$

$$\sigma_{12}(0,x_2,x_3) = -(7057723076923077x_3(x_2-1))/262144$$

$$\sigma_{13}(0,x_2,x_3) = -(7057723076923077(x_2-1)(x_3-1))/262144$$

Right edge surface, $x_1 = a = 1$

$$\sigma_{11}(a,x_2,x_3) = (1323323076923077x_2)/32768 + (1543876923076923x_2x_3)/16384 - 1323323076923077/32768$$

$$\sigma_{12}(a,x_2,x_3) = (7057723076923077x_2x_3)/262144$$

$$\sigma_{13}(a,x_2,x_3) = (7057723076923077x_2)/262144 + (7057723076923077(x_2-1)(x_3-1))/2621444$$

Back surface, $x_2 = 0$

$$\sigma_{12}(x_1,0,x_3) = -(7057723076923077x_3(x_1-1))/262144$$

$$\sigma_{22}(x_1,0,x_3) = (1323323076923077x_1)/32768 - (1543876923076923x_3(x_1-1))/16384$$

$$\sigma_{23}(x_1,0,x_3) = (7057723076923077x_1)/262144 - (7057723076923077x_1(x_3-1))/262144 - 7057723076923077/262144$$

Front surface, $x_2 = b = 1$

$$\sigma_{12}(x_1,b,x_3) = (7057723076923077x_1x_3)/262144$$

$$\sigma_{22}(x_1,b,x_3) = (1323323076923077x_3)/32768 + (1543876923076923x_3(x_1-1))/16384$$

$$\sigma_{23}(x_1,b,x_3) = (7057723076923077x_1(x_3-1))/262144$$

Bottom surface, $x_3 = 0$

$$\sigma_{13}(x_1, x_2, 0) = (7057723076923077x_2)/262144 - (7057723076923077x_1x_2)/262144 - 7057723076923077/262144$$

$$\sigma_{23}(x_1, x_2, 0) = (7057723076923077x_1)/262144 - (7057723076923077(x_1 - 1)(x_2 - 1))/262144$$

$$\sigma_{33}(x_1, x_2, 0) = -(1543876923076923x_1(x_2 - 1))/16384$$

Top surface, $x_3 = h$

$$\sigma_{13}(x_1, x_2, h) = (7057723076923077x_1x_2)/262144 - (63519507692307693x_2)/2621440 + 63519507692307693/2621440$$

$$\sigma_{23}(x_1, x_2, h) = (7057723076923077(x_1 - 1)(x_2 - 1))/262144 - (63519507692307693x_1)/2621440$$

$$\sigma_{33}(x_1, x_2, h) = (1323323076923077x_1)/327680 + (1323323076923077x_2)/327680 + (1543876923076923x_1(x_2 - 1))/16384 - 1323323076923077/327680$$

References

Barlow, J. (1976). Optimal stress locations in finite element models. *International Journal for Numerical Methods in Engineering, 10*(2), 243–251.

Batra, R. C., & Liang, X. Q. (1997). Finite dynamic deformations of smart structures. *Computational Mechanics, 20*(5), 427–438.

Batra, R. C., & Love, B. M. (2005). Mesoscale analysis of shear bands in high strain rate deformations of tungsten/nickel-iron composites. *Journal of Thermal Stresses, 28*(6-7), 747–782.

Becker, E. B., Carey, G. F., & Oden, J. T. (1981). *Finite elements, an introduction*. Englewood Cliffs: Prentice-Hall, Inc.. Vol. I.

Carrera, E. (2000). *A priori* vs. *a posteriori evaluation of transverse stresses in multilayered orthotropic plates*. *Composite Structures, 48*, 245–260.

Chaudhuri, R. A., & Seide, P. (1987). An approximate semi-analytical method for prediction of interlaminar shear stresses in an arbitrarily laminated thick plate. *Computers & Structures, 25*(4), 627–636.

Gere, J. M., & Timoshenko, S. P. (1990). *Mechanics of materials* (3rd Edition). Boston: PWS-Kent Publishing Co.

Kant, T., & Swaminathan, K. (2000). Estimation of transverse/interlaminar stresses in laminated composites – a selective review and survey of current developments. *Composite Structures, 49*(1), 65–75.

Kellog, O. D. (1953). *Foundations of potential theory*. New York: Dower Publications.

Murakami, H. (1986). Laminated composite plate theory with improved in-plane responses. *Journal of Applied Mechanics, 53*(3), 661–666.

Noor, A. K., Burton, W. S., & Peters, J. M. (1990). Predictor-corrector procedures for stress and free vibration analyses of multilayered composite plates and shells. *Computer Methods in Applied Mechanics and Engineering, 82*(1), 341–363.

Park, J. W., & Kim, Y. H. (2002). Re-analysis procedure for laminated plates using FSDT finite element model. *Computational Mechanics, 29*(3), 226–242.

Park, J. W., Lee, K. C., & Kim, Y. H. (2003). Comparative study of finite element based response evaluation methods for laminated plates. *Computational Mechanics, 32*(1), 115–133.

Reissner, E. (1984). On a certain mixed variational theorem and a proposed application. *International Journal for Numerical Methods in Engineering, 20*(7), 1366–1368.

Rohwer, K., Friedrichs, S., & Wehmeyer, C. (2005). Analyzing laminated structures from fibre-reinforced composite material: An assessment. *Technische Mechanik-European Journal of Engineering Mechanics, 25*(1), 59–79.

Srinivas, S., & Rao, A. K. (1970). Bending, vibration and buckling of simply supported thick orthotropic rectangular plates and laminates. *International Journal of Solids and Structures, 6*(11), 1463–1481.